JOURNAL OF SOLID STATE CHEMISTRY 114, 359–363 (1995)

Hydrothermal Synthesis and Crystal Structure of a Novel Barium Vanadium Oxide: $Ba_{0.4}V_3O_8(VO)_{0.4} \cdot nH_2O$

Yoshio Oka, Osamu Tamada,* Takeshi Yao,† and Naoichi Yamamoto*

*Department of Natural Environment Sciences, Faculty of Integrated Human Studies, *Graduate School of Human and Environmental Studies, and †Division of Energy and Hydrocarbon Chemistry, Graduate School of Engineering, Kyoto University, Kyoto 606, Japan*

Received February 14, 1994; in revised form April 20, 1994; accepted April 25, 1994

A new barium vanadium oxide $Ba_{0.4}V_3O_8(VO)_{0.4} \cdot nH_2O$ ($n \sim 0.6$) has been synthesized hydrothermally from a $VOCl_2$–$BaCl_2$ solution. The green–black crystal composed of elongated thin plates exhibits a monoclinic system: $P2_1/m$, $a = 10.153(3)$ Å, $b = 3.6329(9)$ Å, $c = 9.435(2)$ Å, and $\beta = 102.10(2)°$. Structural analysis using 951 independent reflections led to $R = 0.063$ and $R_w = 0.076$. The structure is basically a layered type made up of V_3O_8 layers with interstitial Ba^{2+} ions and water molecules. Its striking feature is that the V_3O_8 layers are bridged imperfectly by partially absent VO_5 trigonal bipyramids which form tunnel-like openings. The structure is thus regarded as an intermediate between layered and tunnel structure types. Interstitial Ba^{2+} ions were observed to be displaced from the position on the mirror plane.

INTRODUCTION

Vanadium (IV, V) oxide bronzes crystallize in structures consisting of V–O polyhedral frameworks with foreign cations located in the interstitial sites (1). Extensive studies have revealed several structural types of V–O polyhedral frameworks which offer interstitial sites for foreign cations. The structural types can be classified into layered and tunnel types: for example, a layered-type V_2O_5 framework in δ-$M_xV_2O_5$ (2) and a tunnel-type V_2O_5 framework in β-$M_xV_2O_5$ (3), where M denotes interstitial cations of generally mono- or divalent states. We report here a new barium vanadium oxide of this category with a novel structure that has been synthesized in the Ba–V–O hydrothermal system. The structure is distinguished by a V–O polyhedral framework which exhibits a structure intermediate between layered and tunnel structure types. That is, the structure is composed of V–O octahedral layers that are intermittently bridged by V–O polyhedra forming tunnel-like cavities.

SAMPLE PREPARATION

The starting materials in the present Ba–V–O hydrothermal system were vanadyl chloride and barium chloride. A solution of 80 mM $VOCl_2$ to which $BaCl_2$ was added until a Ba/V molar ratio of 0.2 was reached was sealed in a Pyrex ampoule and treated hydrothermally at 240°C for 24 hr. Dark-green fibrous precipitates were filtered out and washed thoroughly with distilled water. Single crystals shaped like elongated thin plates were separated from the precipitates. The compositional analyses were performed as follows. The Ba to V molar ratio was determined by a Phillips PV9900 EDAX system, the oxidation number of V was determined by the light absorptiometry of V(IV) and V(V) ionic species dissolved in an acidic solution (4), and the water content was obtained by conventional thermogravimetric (TG) analysis.

SINGLE-CRYSTAL X-RAY ANALYSIS

The data were collected from a single crystal of dimensions 0.33 × 0.05 × 0.01 mm using a Rigaku AFC-5S diffractometer with monochromatized Mo$K\alpha$ radiation. The crystal system is monoclinic, and the cell parameters as determined using 24 reflections in $41 \leq 2\theta \leq 54°$ are $a = 10.153(3)$ Å, $b = 3.6329(9)$ Å, $c = 9.435(2)$ Å, and $\beta = 102.10(2)°$. The shape of the single crystal is shown in Fig. 1, where the long side corresponds to the b-axis. Systematic extinction was confirmed for $0k0$ reflections with odd k, yielding possible space groups of $P2_1$ and $P2_1/m$. The centrosymmetric $P2_1/m$ was chosen for the structural analysis. Intensity data were collected for 1763 independent reflections with $2\theta \leq 70°$. The intensity fluctuations were monitored to be less than 3% by measuring standard reflections of 322, 612, and 320 every 200 reflections. An empirical correction of the absorption effect was made around the b-axis (long axis) using the Furnus method (5). The low-intensity reflections showed rather small S–N ratios due to the tiny size of the crystal, and hence 951 reflections with $|F_0| > 6\sigma$ were used in the structure refinement. The crystallographic data and experimental parameters are listed in Table 1.

0022-4596/95 $6.00

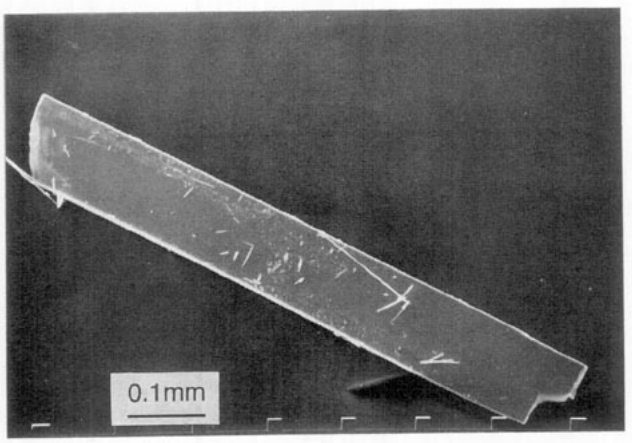

FIG. 1. Scanning electron micrograph of a single crystal of $Ba_{0.4}V_3O_8(VO)_{0.4} \cdot nH_2O$.

STRUCTURE DETERMINATION

The compound was identified by compositional analyses as a hydrated barium vanadium oxide with an atomic ratio Ba : V : O = 0.110(5) : 1 : 2.46(1) and a water content ~3.0 wt%. The dehydration process was completed below 300°C, suggesting the presence of interstitial water molecules.

The structure determination was conducted by the Patterson and Fourier methods using the program FRAXY (6). The analysis of the Patterson maps gave a model of a layered-type structure consisting of V_3O_8 layers and interstitial Ba atoms. The structure refinement was performed using the program RADY (7) with atomic scattering factors for neutarl atoms from the "International Tables for X-Ray Crystallography IV" (8). The refinement based on the model yielded $R = 0.25$ and the composition $Ba_{0.37}V_3O_8$ (Ba : V : O = 0.12 : 1 : 2.67). Fourier maps were synthesized at this stage, and two unidentified peaks were detected in the interlayer region. They were assigned to partially filled V and O sites (V(4) and O(9)). Occupancies for both sites were determined independently and showed nearly the same values, 0.420(5) for V(4) and 0.43(2) for O(9), and the V(4)–O(9) separation was determined to be 1.63(3) Å, indicating the formation of a V(4)–O(9) bonding unit. The Fourier profile for the interstitial atoms is significantly elongated along the *b*-axis, as shown in Fig. 2 for the *yz* section at $x = 0.59$, showing a summit of the Fourier peak (Fig. 2a), and that at $x = 0.57$, showing a channel linking the Fourier peaks (Fig. 2b). The profile represents the distribution of interstitial Ba atoms and water molecules. For the sake of profile fitting, the Ba atom was rearranged into two 4*f* positions (Ba(1) and Ba(2)) from the 2*e* position and the position of the water molecule ($O_w(10)$) was set in the channel as depicted in Fig. 2b. It is noted that the $O_w(10)$ site as well as the Ba(1) and Ba(2) sites do not necessarily indicate a unique position of the water molecule. The structural refinement based on the revised model led to $R = 0.063$ and $R_w = 0.076$. The final atomic parameters, isotropic temperature factors, and site occupancies are listed in Table 2, and the anisotropic thermal parameters in Table 3. The crystal structure is depicted in Fig. 3. The composition becomes $Ba_{0.37}V_3O_8(VO)_{0.42} \cdot 0.41H_2O$, which gives the atomic ratio Ba : V : O = 0.11 : 1 : 2.46, in good agreement with that from the compositional analyses. The water content from the TG analysis corresponds to a value of $\sim 0.6H_2O$; it is alterable depending on the environment.

TABLE 1
Crystal Data and Experimental Parameters

Chemical formula	$Ba_{0.37}V_3O_8(VO)_{0.42} \cdot 0.41H_2O$
Crystal systesm	Monoclinic
Space group	$P2_1/m$ ($P2_1$)
a (Å)	10.153(3)
b (Å)	3.6329(9)
c (Å)	9.435(2)
β (°)	102.10(2)
Z	2
D_c (g cm^{-3})	3.58
Crystal size (mm)	0.33 × 0.05 × 0.01
Radiation	Mo$K\alpha$
Scan technique	$2\theta - \omega$
Scan width (°)	$\Delta\omega = 1.3 + 0.3 \tan\theta$
Scan speed (degrees min^{-1})	4
2θ range (°)	0–70
No. unique reflections ($\|F_0\|>0$)	1763
No. unique reflections ($\|F_0\|>6\sigma$)	951
No. parameters	179
R	0.063
R_w	0.076

DESCRIPTION OF THE CRYSTAL STRUCTURE

The compound is represented by $Ba_{0.4}V_3O_8(VO)_{0.4} \cdot nH_2O$ or in general by $Ba_xV_3O_8(VO)_y \cdot nH_2O$. The bond distances and angles for $V(1)O_5$, $V(2)O_6$, $V(3)O_6$, and $V(4)O_5$ polyhedra are listed in Table 4, and the V–V distances in Table 5. The structure is primarily made up of V_3O_8 layers as demonstrated in Fig. 3 by the solid-line framework. The V_3O_8 layer is found to be isostructural with that of $H_2V_3O_8$ (9) and thus closely related to the V–O framework of β-$M_xV_2O_5$ (3). The V_3O_8 layers are bridged by $V(4)O_5$ trigonal bipyramids, forming tunnel-like cavities, but it is worth noting that the bridging is imperfect because about 60% of the $V(4)O_5$ bipyramids are absent. Therefore, the structure is not of an ideal layered or tunnel type but is intermediate between both types.

The oxidation number of V is 4.70, and about 30% of

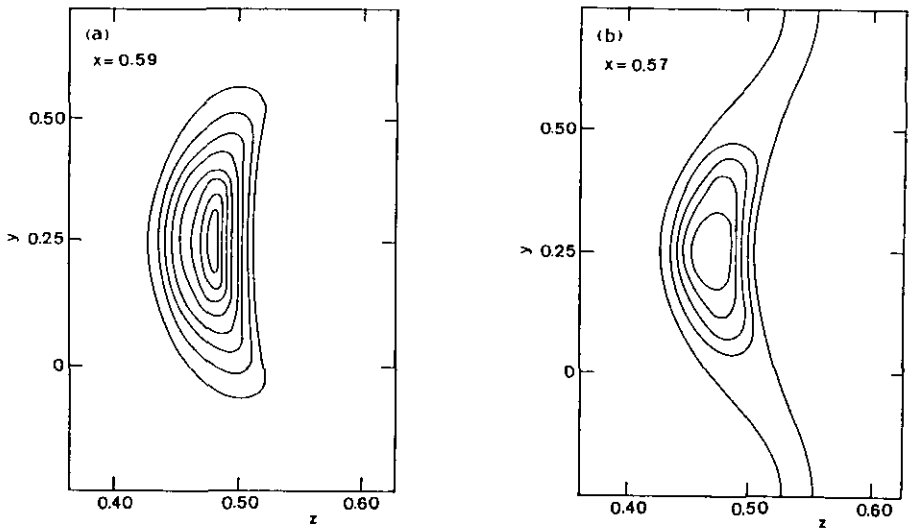

FIG. 2. Fourier contour maps for the Ba atom in the yz sections at (a) $x = 0.59$ and (b) $x = 0.57$. Contours are drawn at an interval of $5e/Å^3$.

V atoms are V^{4+} ions. The distribution of V^{4+} ions is determined on the basis of ionic radii sums and bond-strength calculations. The average V–O distances in the VO_5 bipyramid are 1.841 Å for V(1) and 1.862 Å for V(4), and those in the VO_6 octahedron are 1.943 Å for V(2) and 1.938 Å for V(3). They are compared with the sums of $V^{4+,5+}$ and O^{2+} ionci radii (10): 1.99, 1.94, and 1.86 Å for $V^{4+}(6)$, $V^{5+}(6)$, and $V^{5+}(5)$, respectively, where the coordination number is given in parentheses. Consequently all the V sites seem to be V^{5+}-like, and so V^{4+} ions are not concentrated in one particular site. In addition, the V–O bond strength s for a bond distance d is calculated using $s = 21.29d^{-5.0} - 0.153$, derived specifically for the vanadium oxide compounds (11). The sums of bond strengths for V(1), V(2), V(3), and V(4) are 4.77, 4.53, 4.58, and 4.94, respectively. These values suggest that V^{4+} ions prefer the V(2) and V(3) sites and the V(4) site is more V^{5+}-like.

The partially absent $V(4)O_5$ bipyramid is a distinguishing feature of the structure and plays a role in stabilizing the V_3O_8 layer as discussed in the following. The bond strengths of O atoms in the V_3O_8 layer before the $V(4)O_5$ bipyramid is introduced are given in Table 6. The O(2) atom shows an unusually low value of 0.61, while other O atoms have adequate values of 1.8 ~ 2.0. This arises from the fact that O(2) bonds solely to V(2) at a distance of 1.946 Å, and thus the V_3O_8 layer alone is structurally unstable in terms of the oxygen charge balance. The same problem in the V_3O_8 layer of $H_2V_3O_8$ is solved by adding

TABLE 2
Atomic Parameters, Isotropic Temperature Factors, and Site Occupancies for $Ba_{0.4}V_3O_8(VO)_{0.4} \cdot nH_2O$

Atom	Position	x	y	z	B_{eq} (Å^2)	Occupancy
V(1)	2e	0.5932(2)	¼	0.9380(2)	0.68(4)	1.0
V(2)	2e	0.8496(2)	¼	0.1946(2)	0.88(4)	1.0
V(3)	2e	0.9152(2)	¼	0.8651(2)	0.63(4)	1.0
V(4)	2e	0.0485(5)	¼	0.5595(4)	0.97(9)	0.420(5)
Ba(1)[a]	4f	0.5876(5)	0.30	0.4686(6)	2.0(3)	0.091(2)
Ba(2)[a]	4f	0.598(1)	0.404(4)	0.4804(10)	6.1(8)	0.095(3)
O(1)	2e	0.6979(8)	¼	0.2206(10)	1.6(2)	1.0
O(2)	2e	0.9545(13)	¼	0.3925(10)	2.7(3)	1.0
O(3)	2e	0.7785(7)	¼	0.9783(8)	0.7(2)	1.0
O(4)	2e	0.8179(8)	¼	0.7068(9)	1.3(2)	1.0
O(5)	2e	0.0380(8)	¼	0.0974(8)	0.8(2)	1.0
O(6)	2e	0.0962(8)	¼	0.8055(9)	1.1(2)	1.0
O(7)	2e	0.5538(9)	¼	0.7657(9)	1.4(2)	1.0
O(8)	2e	0.4236(8)	¼	0.0089(9)	1.0(2)	1.0
O(9)	2e	0.199(2)	¼	0.523(2)	2.1(5)	0.43(2)
$O_w(10)$[a]	4f	0.433(3)	0.330(14)	0.461(3)	5(3)	0.20(3)

[a] Placed for fitting the Fourier profile of the interstitial atoms (see text).

TABLE 3
Anisotropic Thermal Parameters U_{ij} (Å^2) for $Ba_{0.4}V_3O_8(VO)_{0.4} \cdot nH_2O$

Atom	U_{11}	U_{22}	U_{33}	U_{12}	U_{13}	U_{23}
V(1)	0.0088(2)	0.004(1)	0.0136(2)	0	0.0037(1)	0
V(2)	0.0109(2)	0.008(1)	0.0155(2)	0	0.0049(1)	0
V(3)	0.0091(2)	0.004(1)	0.0113(2)	0	0.0027(1)	0
V(4)	0.0247(5)	0.004(2)	0.0080(4)	0	0.0019(3)	0
Ba(1)	0.0089(4)	0.06(1)	0.013(4)	0.001(2)	0.0039(4)	0.000(2)
Ba(2)	0.089(2)	0.11(3)	0.02(1)	−0.007(5)	−0.008(1)	0.025(4)
O(1)	0.0112(7)	0.024(7)	0.0315(9)	0	0.0126(8)	0
O(2)	0.061(2)	0.009(6)	0.025(1)	0	−0.008(1)	0
O(3)	0.0070(6)	0.005(4)	0.0126(7)	0	0.0018(5)	0
O(4)	0.0112(7)	0.017(6)	0.0168(8)	0	0.0013(7)	0
O(5)	0.0137(7)	0.001(4)	0.0151(8)	0	0.0055(6)	0
O(6)	0.0159(7)	0.006(5)	0.0196(8)	0	0.0049(7)	0
O(7)	0.0142(7)	0.018(6)	0.0208(9)	0	0.0038(7)	0
O(8)	0.0098(7)	0.006(5)	0.0232(9)	0	0.0086(8)	0
O(9)	0.063(3)	0.01(1)	0.020(2)	0	0.025(2)	0
$O_w(10)$	0.025(3)	0.14(9)	0.023(3)	−0.05(1)	−0.017(3)	0.07(2)

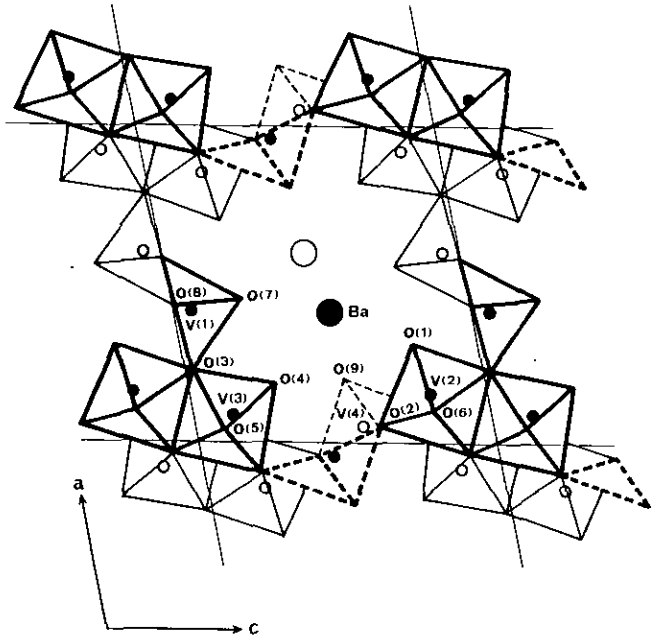

FIG. 3. Crystal structure of $Ba_{0.4}V_3O_8(VO)_{0.4} \cdot nH_2O$ viewed along the *b*-axis. Large and small circles denote Ba and V atoms, respectively, at $y = \frac{1}{4}$ (open circles) and $y = \frac{3}{4}$ (closed circles). The framework of the V_3O_8 layer is drawn by solid lines, and that of the partially absent VO_5 bipyramid by broken lines.

hydrogen atoms to the O atom in question, where the hydrogen atoms play a further role in joining the V_3O_8 layers through hydrogen bonds (9). In the present case, the charge balance of O(2) is attained by introducing a V(4) atom together with an O(9) atom, forming a $V(4)O_5$ bipyramid. The O(2) is now coordinated by two V(4) at $y = \frac{3}{4}$ and $-\frac{1}{4}$ (1.874 Å) and one V(4) at $y = \frac{1}{4}$ (1.662 Å) in addition to one V(2). Taking into account the V(4) occupancy of 0.42, the average bond strength of O(2) becomes an adequate value of 1.90. It is thought that the $V(4)O_5$ bipyramid is indispensable for the stabilization of the V_3O_8 layer. Since the V(4)–V(4) distance of 2.250 Å (Table 5) is too short for the V–V separation, the V(4) site next to a filled V(4) site must be vacant, implying that the O(2) is coordinated in practice by two V(4) at $y = \frac{3}{4}$ or one V(4) at $y = \frac{1}{4}$. The row of $V(4)O_5$ bipyramids along the *b*-axis lacks any periodic relationship to other rows, as is clear from the lattice period of the *b*-axis. This is the first example of partially absent V–O polyhedra in the complex vanadium (IV, V) oxides.

The compound accommodates interstitial Ba^{2+} ions with a site occupancy of 0.37. The Fourier profile for the Ba atom (Fig. 2) is elongated along the *b*-axis, indicating displacement from the 2*e* position on the mirror plane. Similar elongated Fourier profiles have been reported for some interstitial cations in the hollandite-type structures (12–16). For example, a Rb^+ ion in $Rb_{1.5}Mn_8O_{16}$ hollandite exhibits an elongated profile in the 2×2 MnO_6 octahedral tunnel (12). In $Ba_{0.4}V_3O_8(VO)_{0.4} \cdot nH_2O$, assuming the summit of the Fourier peak to be the Ba site instead of the Ba(1) and Ba(2) sites, the Ba site is surrounded by

TABLE 4
Bond Distances (Å) and Angles (°) for VO_6 Octahedra and VO_5 Trigonal Bipyramids in $Ba_{0.4}V_3O_8(VO)_{0.4} \cdot nH_2O$

$V(1)O_5$ trigonal bipyramid			
V(1)–O(3)	1.840(7)	V(1)–O(7)	1.591(8)
V(1)–O(8)	1.973(9)	V(1)–O(8)[a]	1.901(3) ×2
O(3)–V(1)–O(7)	103.8(3)	O(3)–V(1)–O(8)	149.0(3)
O(3)–V(1)–O(8)[a]	95.2(2)	O(7)–V(1)–O(8)	107.3(4)
O(7)–V(1)–O(8)[a]	104.6(3)	O(8)–V(1)–O(8)[a]	77.2(5)
O(8)[a]–V(1)–O(8)[a]	145.6(2)		
$V(2)O_6$ octahedron			
V(2)–O(1)	1.610(9)	V(2)–O(2)	1.946(10)
V(2)–O(3)	2.017(7)	V(2)–O(5)	2.288(9)
V(2)–O(6)[a]	1.898(3) ×2		
O(1)–V(2)–O(2)	101.7(5)	O(1)–V(2)–O(3)	90.2(4)
O(1)–V(2)–O(5)	165.5(4)	O(1)–V(2)–O(6)[a]	106.7(3)
O(2)–V(2)–O(3)	168.1(5)	O(2)–V(2)–O(5)	92.8(4)
O(2)–V(2)–O(6)[a]	84.3(3)	O(3)–V(2)–O(5)	75.3(3)
O(3)–V(2)–O(6)[a]	92.4(3)	O(5)–V(2)–O(6)[a]	74.5(3)
O(6)[a]–V(2)–O(6)[a]	146.3(4)		
$V(3)O_6$ octahedron			
V(3)–O(3)	1.920(8)	V(3)–O(4)	1.609(8)
V(3)–O(5)	2.282(7)	V(3)–O(5)[a]	1.892(2) ×2
V(3)–O(6)	2.031(9)		
O(3)–V(3)–O(4)	98.1(4)	O(3)–V(3)–O(5)	77.3(3)
O(3)–V(3)–O(5)[a]	94.5(3)	O(3)–V(3)–O(6)	162.8(3)
O(4)–V(3)–O(5)	175.4(4)	O(4)–V(3)–O(5)[a]	104.7(2)
O(4)–V(3)–O(6)	99.1(4)	O(5)–V(3)–O(5)[a]	75.9(2)
O(5)–V(3)–O(6)	85.5(3)	O(5)[a]–V(2)–O(5)[a]	147.5(3)
O(5)[a]–V(3)–O(6)	81.1(3)		
$V(4)O_5$ trigonal bipyramid			
V(4)–O(2)	1.662(10)	V(4)–O(2)[a]	1.874(3) ×2
V(4)–O(6)	2.269(9)	V(4)–O(9)	1.633(26)
O(2)–V(4)–O(2)[a]	101.2(5)	O(2)–V(4)–O(6)	80.4(5)
O(2)–V(4)–O(9)	100.3(8)	O(2)[a]–V(4)–O(2)[a]	151.5(3)
O(2)[a]–V(4)–O(6)	76.0(3)	O(2)[a]–V(4)–O(9)	96.6(5)
O(6)–V(4)–O(9)	101.9(8)		

[a] Symmetry code: $-x, \frac{3}{4}, -z$.

TABLE 5
V–V Distances (Å) in $Ba_{0.4}V_3O_8(VO)_{0.4} \cdot nH_2O$

V(1)–V(1)[a]	3.029(2)	V(1)–V(2)	3.161(3)
V(1)–V(3)	3.480(3)	V(2)–V(3)	3.313(3)
V(2)–V(3)[a]	3.144(2)	V(2)–V(4)[a]	2.958(4)
V(3)–V(4)	3.433(5)	V(4)–V(4)[a]	2.251(4)

[a] Symmetry code: $-x, \frac{3}{4}, -z$.

TABLE 6
Bond Strengths for V and O Atoms in the Structure of the V_3O_8 Layer

Atom	O(1)	O(2)	O(3)	O(4)	O(5)	O(6)	O(7)	O(8)	Total
V(1)			0.86				1.94	1.97	4.77
V(2)	1.82	0.61	0.49		0.19	1.42			4.53
V(3)			0.66	1.82	1.64	0.46			4.58
Total	1.82	0.61	2.01	1.82	1.83	1.87	1.94	1.97	

TABLE 7
Bond Distances (Å) for Ba–O Polyhedron in $Ba_{0.4}V_3O_8(VO)_{0.4} \cdot nH_2O$

Ba[a]–O(1)	2.818(6)	Ba–O(4)	2.817(7)
Ba–O(7)	2.859(8)	Ba–O(7)[b]	3.038(8) ×2
Ba–O(9)[b]	2.783(12) ×2		

[a] Ba atom is placed at the summit of the Fourier peak (Fig. 2a): (0.590, 0.25, 0.475).
[b] Symmetry code: $-x, \frac{3}{4}, -z$.

seven oxygens as depicted in Fig. 4. The Ba–O distances are listed in Table 7. As the Ba atom is coordinated by two O(9) at $y = \frac{3}{4}$ at the shortest distance, the Ba–O(9) interaction should be predominant in the Ba–O polyhedron. The O(9) sites along the *b*-axis must be occupied nearly alternately because the $V(4)O_5$ bipyramids are prohibited from adjoining, indicating that the two O(9) sites in Fig. 4 are, in most cases, simultaneously occupied or vacant. The Ba site with filled O(9) sites on each side is therefore preferably occupied. Consequently the distribution of the interstitial Ba atoms is similar to that of the $V(4)O_5$ bipyramids.

CONCLUSION

The new compound, $Ba_{0.4}V_3O_8(VO)_{0.4} \cdot nH_2O$, was hydrothermally synthesized from a $VOCl_2$–$BaCl_2$ solution. The structure is basically a layered type composed of V_3O_8 layers with interstitial Ba^{2+} ions. The V_3O_8 layer is structurally related to the V–O frameworks of β-$M_xV_2O_5$ (3) or $H_2V_3O_8$ (9). The striking feature of the structure is the partially absent VO_5 bipyramids which bridge and stabilize the V_3O_8 layers. The structure is thus regarded as an intermediate between layered and tunnel types. The interstitial Ba atom is displaced from the position on the mirror plane and interacts with the apical oxygens of the partially absent VO_5 bipyramids.

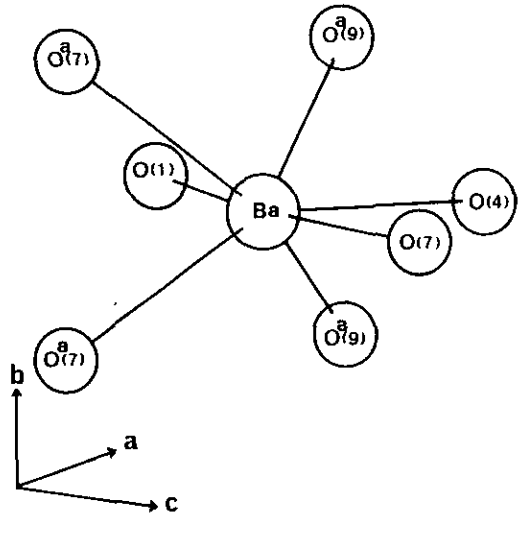

FIG. 4. Coordination of the Ba atom with oxygens. The Ba atom is placed at the summit of the Fourier peak shown in Fig. 2a, and O atoms denoted by O^a are at $y = \frac{3}{4}$.

ACKNOWLEDGMENT

We are grateful to Professor S. Sasaki of the Tokyo Institute of Technology for preparing and revising the computer programs.

REFERENCES

1. P. Hagenmuller, *Prog. Solid State Chem.* **5,** 71 (1971).
2. S. Anderson, *Acta. Chem. Scand.* **19,** 1371 (1965).
3. A. D. Wadsley, *Acta. Crystallogr.* **8,** 695 (1955).
4. Y. Oka, N. Yamamoto, T. Ohtani, and T. Takada, *J. Ceram. Soc. Jpn.* **97,** 1441 (1989).
5. A. C. North, D. C. Phillips, and F. S. Mathews, *Acta Crystallogr. Sect. A* **24,** 351 (1968).
6. S. Sasaki, private communication.
7. S. Sasaki, KEK Internal Report, Vol. 3. National Laboratory of High Energy Physics, Tukuba, 1987.
8. "International Tables for X-Ray Crystallography IV." Kynoch Press, Birmingham, UK, 1974.
9. Y. Oka, T. Yao, and N. Yamamoto, *J. Solid State Chem.* **89,** 372 (1990).
10. R. D. Shannon and C. T. Prewitt, *Acta Crystallogr. Sect. B* **25,** 925 (1969).
11. K. Walterson, "Chem. Commun. Univ. Stockholm No. 7," 1976.
12. N. Yamamoto, Y. Oka, and O. Tamada, *Mineral. J.* **15,** 41 (1990).
13. M. Watanabe, Y. Fujiki, Y. Kanazawa, and K. Tsukimura, *J. Solid State Chem.* **66,** 56 (1987).
14. O. Tamada and N. Yamamoto, *Mineral. J.* **13,** 130 (1986).
15. J. E. Post, R. B. Von Dreele, and P. R. Buseck, *Acta Crystallogr. Sect. B* **38,** 1056 (1982).
16. W. Sinclair, G. M. McLaughlin, and A. E. Ringwood, *Acta Crystallogr. Sect. B* **36,** 2913 (1980).